AGU PUBLICATIONS

JGR

Journal of Geophysical Research: Space Physics

COMMENTARY

10.1002/2016JA022668

Special Section:
Unsolved Problems in Magnetospheric Physics

Key Points:
- Measurement of 3-D currents in the magnetosphere
- Application in the inner magnetosphere
- Relevance for new MMS measurements

Correspondence to:
M. W. Dunlop,
m.w.dunlop@rl.ac.uk

Citation:
Dunlop, M. W., S. Haaland, P. C. Escoubet, and X.-C. Dong (2016), Commentary on accessing 3-D currents in space: Experiences from Cluster, *J. Geophys. Res. Space Physics*, *121*, 7881–7886, doi:10.1002/2016JA022668.

Received 6 MAR 2016
Accepted 24 JUL 2016
Accepted article online 29 JUL 2016
Published online 12 AUG 2016

Commentary on accessing 3-D currents in space: Experiences from Cluster

M. W. Dunlop[1,4], S. Haaland[2,5], P. C. Escoubet[3], and X.-C. Dong[1]

[1]Space Science Institute, School of Astronautics, Beihang University, Beijing, China, [2]Birkeland Centre for Space Science, University of Bergen, Bergen, Norway, [3]ESA/ESTEC, Noordwijk, Netherlands, [4]RAL Space, STFC, Oxfordshire, UK, [5]Max-Planck Institute for Solar Systems Research, Göttingen, Germany

Abstract The curlometer was introduced to estimate the electric current density from four-point measurements in space; anticipating the realization of the four spacecraft Cluster mission which began full science operations in February 2001. The method uses Ampère's law to estimate current from the magnetic field measurements, suitable for the high-conductivity plasma of the magnetosphere and surrounding regions. The accuracy of the method is limited by the spatial separation knowledge, accuracy of the magnetic field measurement, and the relative scale size of the current structures sampled but nevertheless has proven to be robust and reliable in many regions of the magnetosphere. The method has been applied successfully and has been a key element, in studies of the magnetopause currents; the magnetotail current sheet; and the ring current, as well as allowing other current structures such as flux tubes and field aligned currents to be determined. The method is also applicable to situations where less than four spacecraft are closely grouped or where special assumptions (particularly stationarity) can be made. In view of the new four-point observations of the MMS mission taking place now, which cover a dramatically different spatial regime, we comment on the performance, adaptability, and lessons learnt from the curlometer technique. We emphasize the adaptability of the method, in particular, to the new sampling regime offered by the MMS mission; thereby offering a tool to address open questions on small-scale current structures.

1. The Curlometer

A wide range of currents permeate many regions of space and in particular currents are ubiquitous in the magnetosphere; supporting both large-scale and small-scale plasma structures (in the form of sheets, tubes, and other structures) and connecting different regions. Multiple spacecraft flying in formation often allow spatial gradient estimates of the magnetic field to be made. The four Cluster spacecraft [*Escoubet et al*., 2001] have provided spatial measurements from which a linear calculation of the **curl** of the magnetic field can be made. This "curlometer" estimate [*Dunlop et al*., 1988] provides all components of the electric current density based on the assumption that $\mathbf{curl}(\boldsymbol{B}) = \mu_0 \boldsymbol{J}$ (i.e., using Ampère's law to estimate the average current density in the tetrahedral configuration). The linear, integral form of Ampère's law estimates the average current, J, normal to the face $1ij$ of the tetrahedron from

$$\mu_0 < \boldsymbol{J} > \left(\Delta r_i \Delta R_j\right) = \Delta B_i \times \Delta R_j - \Delta B_j \times \Delta R_i, \text{ e.g., } \mu_0 < \boldsymbol{J} >_{123} \left(\Delta r_{12} \Delta R_{13}\right) = \Delta B_{12} \cdot \Delta R_{13} - \Delta B_{13} \times \Delta R_{12}$$

We also have $<\mathrm{div}(\boldsymbol{B})> |\Delta \boldsymbol{R}_i \cdot \Delta \boldsymbol{R}_{j\wedge} \Delta \boldsymbol{R}_k| = |\sum_{\mathrm{cyclic}} \Delta \boldsymbol{B}_i \cdot \Delta \boldsymbol{R}_{j\wedge} \Delta \boldsymbol{R}_k|$, which estimates indirectly the neglected nonlinear gradients [*Dunlop et al*., 2002; *Robert et al*., 1998]. The shape and size of the spacecraft configuration compared to the relative orientation and scale of the current structures, as well as measurement errors, affect the quality of the estimate; usually indirectly monitored by the quality parameter, $Q = |\mathrm{div}\boldsymbol{B}|/|\mathbf{curl}(\boldsymbol{B})|$. Since $\mathrm{div}\boldsymbol{B}$ should ideally be zero, small values of Q are desirable. Note, however, that $\mathrm{div}\boldsymbol{B}$ is also calculated from gradients in $\boldsymbol{B}$ and thus is restricted by the same constraints as the curl calculations. The value of Q can therefore not be used to derive quantitative error estimates of the current determination.

In the above equations, $\Delta \boldsymbol{B}_{ij}$ and $\Delta \boldsymbol{R}_{ij}$ represent differences in the measured magnetic field and spatial position vectors between spacecraft i and j, respectively. A redundancy in the estimate, since the vector current can be constructed from only three of the faces of the configuration, can be used to verify the sensitivity of the estimate for each component of $\boldsymbol{J}$ (thus indicating uncertainty independently to $\mathrm{div}\boldsymbol{B}$ and hence Q). This original form of the curlometer is identical to the process of directly estimating the linear spatial gradients for each current density component [e.g., *De Keyser et al*., 2007]; for example, from the dyadic of **B**, but the error

handling (and hence relevant quality parameter) is slightly different: in the integral form the estimate is often self-stabilizing.

If the background field contains strong nonlinear gradients (this is the case for the internal geomagnetic field), then the neglect of these gradients in the linear estimates can imply nonphysical currents (the effect is significant in the inner magnetosphere). The solution is to subtract a zero current model field (e.g., IGRF) prior to the curlometer application which is then applied on the residual fields [*Dunlop et al.*, 2015a]. In addition, nonregular tetrahedral configurations preferentially access some components of the current more accurately than others (depending on alignment, or miss-alignment, to the dominant current direction). This can be a significant pitfall to consider when sampling large-scale currents at the magnetopause or magnetotail, for example.

In general terms, these physical errors, require the spatial configuration to be small compared to the current structure to minimize the effect of nonlinear gradients (i.e., nonmeasured gradients in the current density). This requirement, however, is limited by the effect of the measurement errors in $\boldsymbol{B}$ and $\boldsymbol{R}$ and by timing errors between spacecraft. Thus, smaller tetrahedral scales require higher absolute accuracy in $\boldsymbol{B}$ and $\boldsymbol{R}$, and higher temporal behavior requires higher cadence and accuracy of the measurement times. For the smallest Cluster tetrahedron scales (~100 km) measurement uncertainty (~0.1 nT in $\boldsymbol{B}$; few kilometers for $\boldsymbol{R}$ and millisecond timing) was sufficiently low (for currents greater than a few nAm^{-2}) that linearization errors typically dominate the lack of knowledge in the estimates. This is why Q is a reasonable quality indicator. At separations of tens of kilometers (as accessed by the MMS mission, [*Burch et al.*, 2016]) the curlometer is likely to be more often in the linear regime where errors due to gradients in the current density are small. On these spatial scales, however, the measurement errors could become significant unless the currents are large, and all these measurement errors should be minimized. In fact, it is natural that at Cluster separation scales, the curlometer misses small-scale structure and therefore that the estimate will typically be lower than the actual currents. We might expect that on MMS scales, the estimated currents will be larger than comparative measurements by Cluster. At the magnetopause or in the magnetotail, for example, the boundary layer will often be much larger than the MMS separation scales so that substructures can be resolved.

The above summary represents the practical experience gained from the application of the method to Cluster data. It is the purpose of this commentary to illustrate the key pitfalls learnt through applications of which some are shown below. Ready to use implementations of the curlometer method can be obtained from the Cluster Science archive (http://www.cosmos.esa.int/web/csa/software).

2. Applications

The curlometer method has been successful in view of its wide applicability and robustness and has been successfully applied in many different regions of the Earth's magnetosphere, such as the magnetopause [e.g., *Dunlop et al.*, 2002; *Dunlop and Balogh*, 2005; *Haaland et al.*, 2004; *Panov et al.*, 2006]; the magnetotail current sheet [e.g., *Runov et al.*, 2006; *Nakamura et al.*, 2008; *Narita et al.*, 2013]; the ring current and inner magnetosphere [e.g., *Vallat et al.*, 2005; *Shen et al.*, 2014]; field-aligned currents (FAC), [e.g., *Forsyth et al.*, 2008; *Shi et al.*, 2010]; and other transient signatures [e.g., *Roux et al.*, 2015; *Xiao et al.*, 2004; *Shen et al.*, 2008], as well as to structures in the solar wind [e.g., *Eastwood et al.*, 2002].

Recently, the power of the method in returning results for some components of $\boldsymbol{J}$, where less than four spacecraft are available or where assumptions in the behavior of the currents can be made (e.g., stationarity of the field, known FACs or force-free structures), has been explored [e.g., *Vogt et al.*, 2009, 2013; *Shen et al.*, 2012; *Ritter and Lühr*, 2013] as well as the relation to other gradient-based methods [e.g., *Shi et al.*, 2005, 2006; *Dunlop and Eastwood*, 2008]. This is by no means an exhaustive list and the continued usefulness of the curlometer in fact lies in its flexibility of application and formulation. Indeed, the benchmarking of the method can easily be adapted to new regimes, which we briefly describe below.

2.1. The Magnetopause and Tail Current Sheets

One example of curlometer results, shown in Figure 1, is taken from the magnetopause where close comparison with MMS crossings may be carried out and benchmark tests can be done. On 4 November 2003, about 19:05 UT, Cluster traversed the dusk flank magnetopause (position [−6, 16, −7 R_E GSE]) from the magnetosphere into the magnetosheath. The actual crossing of the current sheet only takes about 17 s. Structures

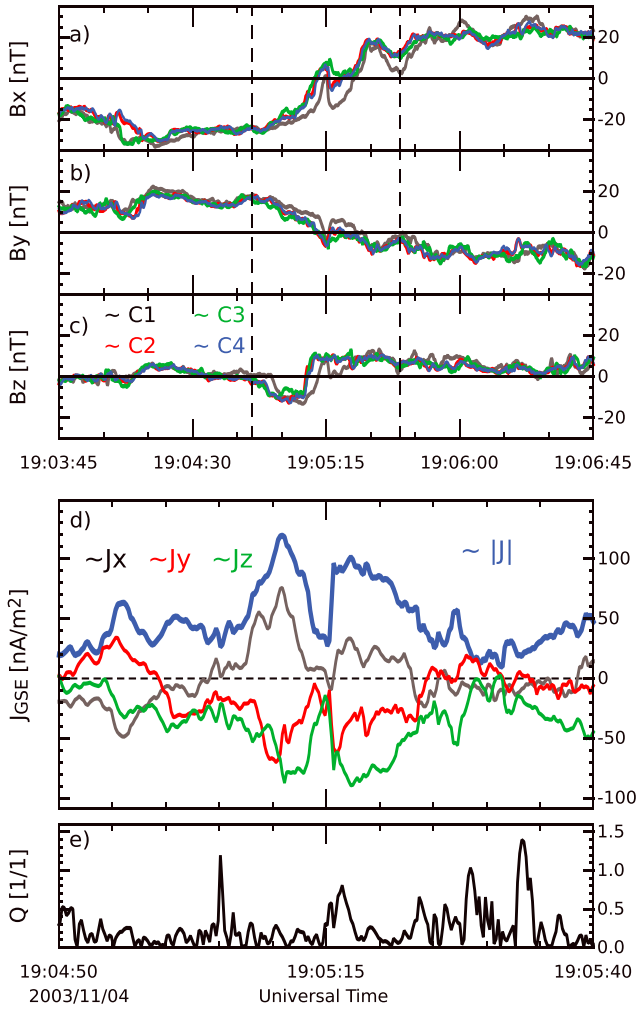

Figure 1. Magnetopause current sheet profile obtained during a duskside magnetopause crossing on 4 November 2003. (a–c) High-resolution GSE components of the magnetic field and (d) the calculated current density, which exhibits a pronounced two-peak structure. (e) The ratio $Q = |\text{div } B| / |\text{curl } B|$, which gives an estimate of the quality of the curlometer current determination [after *Haaland et al.*, 2014].

inside the magnetopause are therefore difficult to resolve in Cluster's plasma measurements which have a 4 s spin resolution, but velocity moments suggest a magnetopause normal velocity of around 35 km/s and thus a current sheet thickness of around 600 km. The individual components of the current, shown in Figure 1e, reveal a layered structure of the magnetopause. The magnetospheric side has a significant *y* component (red line), not present on the magnetosheath side. We interpret this as the signature of two adjacent current sheets, with different current direction. Each current sheet is only a few ion inertial lengths thick.

The magnetotail is another region where the curlometer technique has been successfully applied. Similar layered structures have also been observed there. For example, *Runov et al.* [2006] presented a survey of 30 magnetotail current sheet profiles from the first season of Cluster tail traversals in 2001. In addition to classic current sheets with a single sharp current density maximum, they also found a number of bifurcated current sheets with two quasi-symmetric current density maximums in the northern and southern halves of the plasma sheet, separated by a weaker current layer near the central neutral sheet.

2.2. The Terrestrial Ring Current

The second example is taken from Cluster sampling of the Earth's ring current. Cluster generally crosses the ring current every perigee pass. During the earlier phase of the mission, the polar orbit passed normally through the ring current as was first reported by *Vallat et al.* [2005]. Careful selection of high-quality passes allows a full azimuth scan of the ring current density at all local times [*Zhang et al.*, 2011] (Figure 2) and for a limited radial extent (~4–4.5 R_E). By checking the stability of the current density for each pass, the orientation of the Cluster configuration typically allows the azimuthal (ring plane) component, J_φ, to be estimated accurately. In order to suppress the effect of nonlinear spatial gradients in the Earth's internal field in this region, the IGRF should be subtracted from the measured data so that estimates of the current density are applied to the field residuals [*Shen et al.*, 2014]. MMS will also cover the ring current, and comparisons may be made with the Cluster measurements on MMS scales.

2.3. Variants of the Curlometer With Less Than Four Spacecraft (FACs)

The third example shows the power of the method in situations where less than four point measurements are available. There are two regimes we can test: Cluster distorted configurations, where three spacecraft remain regular or are aligned to the dominant direction of current density, and low Earth orbit (recently covered by the multispacecraft Swarm mission; Figure 3). In the former, three spacecraft may still recover one component normal to the plane of the spacecraft. In the latter, often assumptions of stationarity of the field can

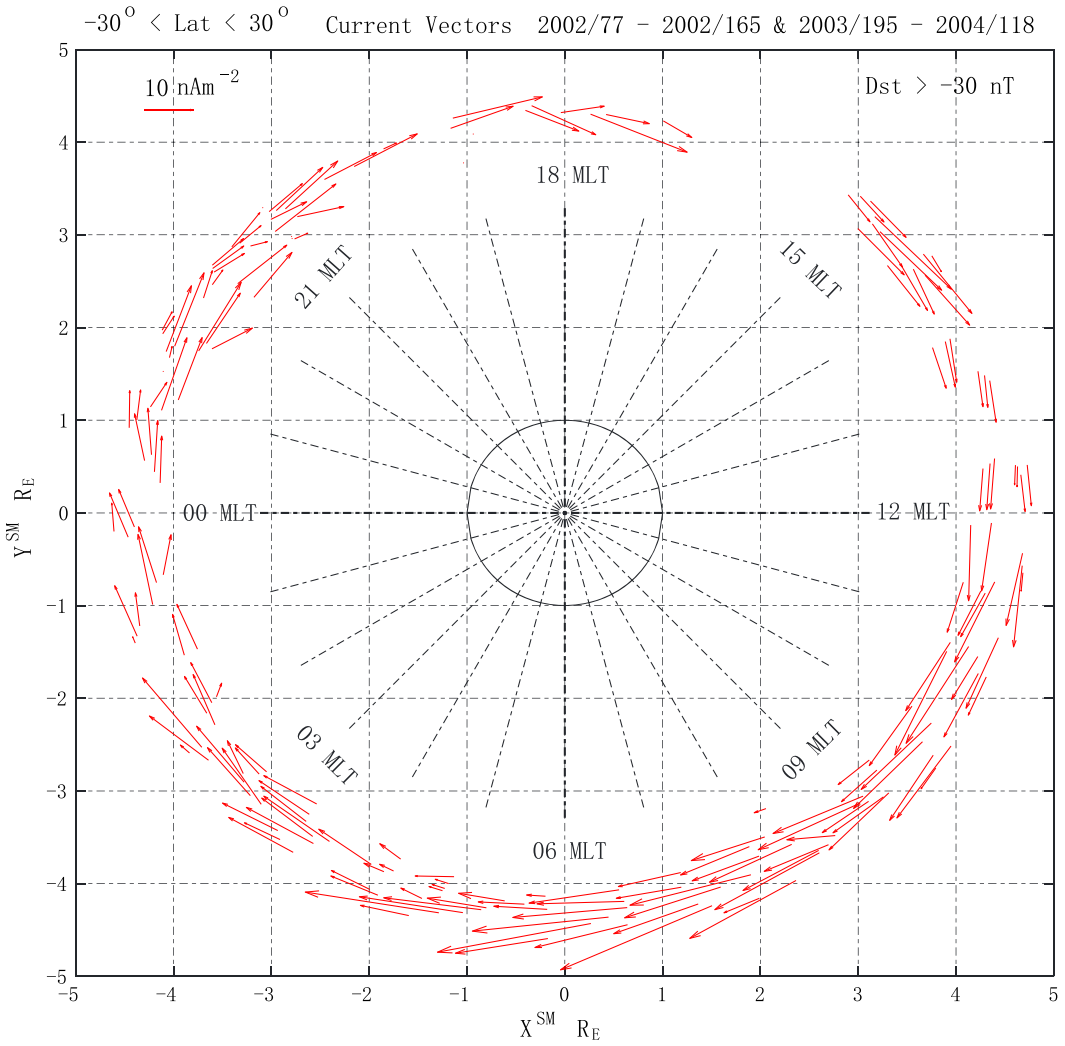

Figure 2. Full azimuth scan (magnetic local time, MLT) of the ring current (RC) passes, plotted in solar magnetic (SM) coordinates (dipole aligned) and between −30° to 30° latitude [*Zhang et al.*, 2011]. The length and direction of the vectors represent 10 min averages of the current density obtained from the curlometer. The measurements represent non-storm ($Dst > -30$ nT) values of the RC. The RC strength is seen to increase with MLT on the dawnside (03–12 MLT) and is a little suppressed on the duskside.

be made so that positions of the spacecraft at adjacent times can be combined to produce added measurement points, allowing the multipoint curlometer to be applied with fewer than four spacecraft. These considerations have been explored in two recent papers [*Dunlop et al.*, 2015a, 2015b], which have estimated the full current density at Swarm altitudes and have shown coordinated field aligned current (FAC) signatures at Cluster and Swarm. In this high field region magnetic residuals are computed by subtracting a high-resolution internal field model.

3. Summary and Challenges for MMS: Small-Scale Structures

For small-scale current structures, spacecraft separation and configuration as well as the ability to filter out magnetic field contributions from other sources will necessarily constrain the applicability of the curlometer method [e.g., *Forsyth et al.*, 2011]. In these circumstances, direct current determination from particle moments may provide comparative estimates, but the measured distributions require carefully checking to ensure that the calculated moments contain all particles contributing to currents. For Cluster, such comparisons have been made [e.g., *Henderson et al.*, 2008; *Petrukovich et al.*, 2015] but are also limited by

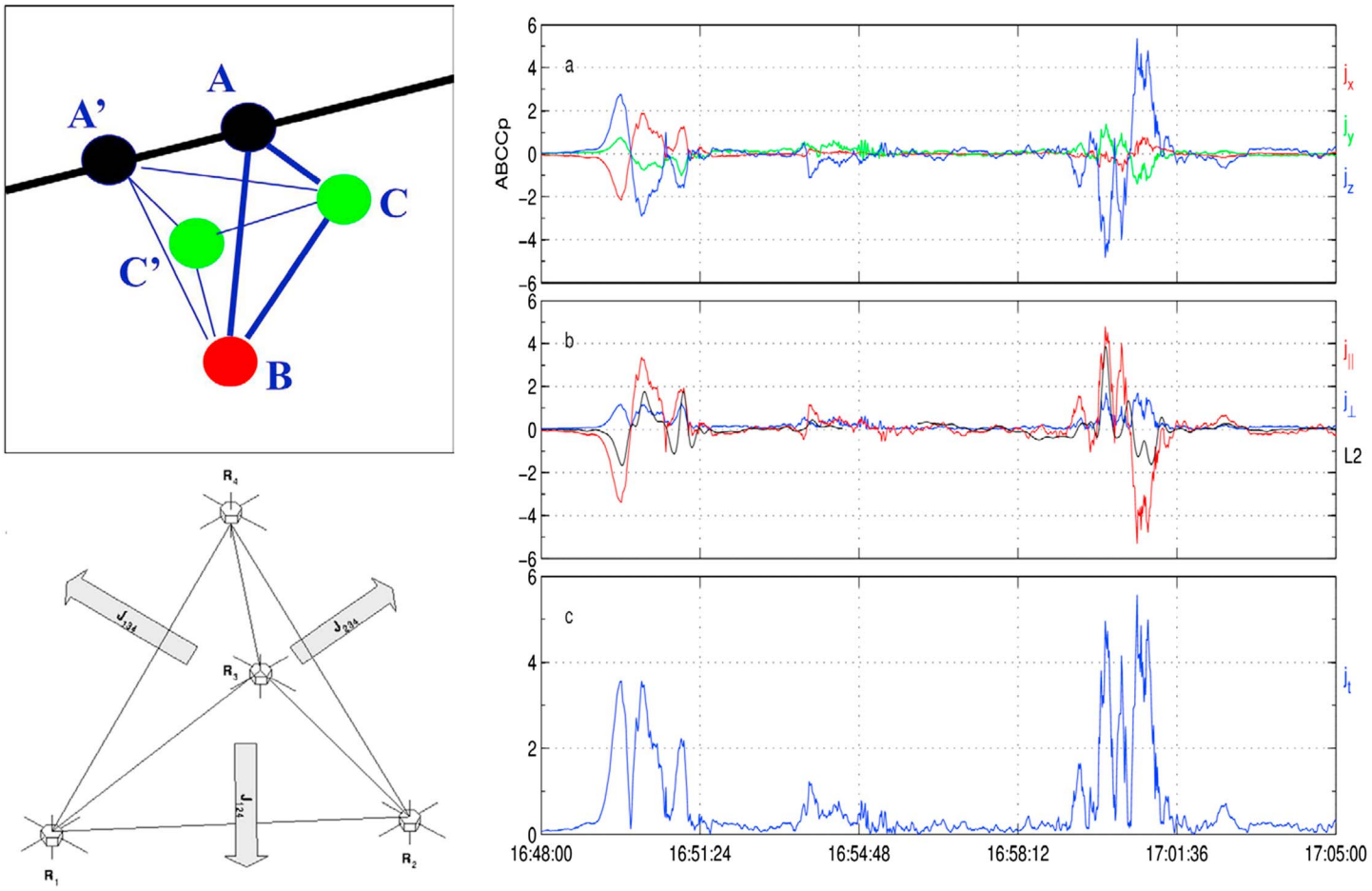

Figure 3. (left column) When three Swarm spacecraft (A, B, C) are grouped closely together, and the positions A′,C′ of these spacecraft a few seconds earlier are combined with A, B, and C, then the full curlometer can be applied, and all components of the current density, ***J***, may be recovered (i.e. by using selected configurations of four spatial positions, e.g., A,A′,B,C). The right-hand plot shows all components of ***J*** (top) for one polar pass where this close grouping occurs, testing the existence of perpendicular currents and hence the assumption of purely field aligned currents (middle panel) [from *Dunlop et al.*, 2015a]. For other times only the Swarm A, C pair remain closely aligned.

the availability (ion moments not available from all four spacecraft (SC)) and time resolution (typically 4 s spin resolution) of the plasma measurements. This is a key combination where we expect new missions like MMS, having plasma instrumentation with the capability for high time resolution measurements, to provide better estimates and new insight on small-scale current structures. Initial results [e.g., *Eastwood et al.*, 2016] are very promising.

Cluster has been in operation for more than 16 years and provided a wealth of information about currents in space. As shown in the few examples above, the curlometer has been a key tool in many of these studies, and the experience gained and lessons learned from Cluster provide a solid foundation for future missions. Moreover, we expect that comparative studies from similar regions, sampled on both large and small scales, will enhance the interpretation of future measurements.

Acknowledgments

All Cluster data, including software implementation of the curlometer, can be obtained from the ESA Cluster Science Archive (http://www.cosmos.esa.int/web/csa/access). M.W.D. is partly supported by an STFC in-house research grant. S.H. was supported by the Norwegian Research Council under grant BCSS 223252.

References

Burch, J. L., T. E. Moore, R. B. Torbert, and B. L. Giles (2016), Magnetospheric multiscale overview and science objectives, *Space Sci. Rev.*, *5*, 1–17, doi:10.1007/s11214-015-0164-9.

De Keyser, J., F. Darrouzet, M. W. Dunlop, and P. M. E. Decreau (2007), Least-squares gradient calculation from multi-point observations of scalar and vector fields: Methodology and applications with Cluster in the plasmasphere, *Ann. Geophys.*, *25*, 971–987, doi:10.5194/angeo-25-971-2007.

Dunlop, M. W., and A. Balogh (2005), Magnetopause current as seen by Cluster, *Ann. Geophys.*, *23*(3), 901–907, doi:10.5194/angeo-23-901-2005.

Dunlop, M. W., and J. P. Eastwood (2008), The curlometer and other gradient based methods, in *Multi-Spacecraft Analysis Methods Revisited*, *ISSI Sci. Rep., SR-008*, edited by G. Paschmann and P. W. Daly, pp. 17–21, Kluwer Academic Pub., Dordrecht, Netherlands.

Dunlop, M. W., D. J. Southwood, K.-H. Glassmeier, and F. M. Neubauer (1988), Analysis of multipoint magnetometer data, *Adv. Space Res.*, *8*, 273–277, doi:10.1016/0273-1177(88)90141-X.

Dunlop, M. W., A. Balogh, K.-H. Glassmeier, and P. Robert (2002), Four-point Cluster application of magnetic field analysis tools: The curlometer, *J. Geophys. Res.*, *107*(A11), 1384, doi:10.1029/2001JA005088.

Dunlop, M. W., et al. (2015a), Multi-spacecraft current estimates at Swarm, *J. Geophys. Res. Space Physics*, *120*, 8307–8316, doi:10.1002/2015JA021707.

Dunlop, M. W., et al. (2015b), Simultaneous field-aligned currents at Swarm and Cluster satellites, *Geophys. Res. Lett.*, *42*, 3683–3691, doi:10.1002/2015GL063738.

Eastwood, J. P., A. Balogh, M. W. Dunlop, and C. W. Smith (2002), Cluster observations of the heliospheric current sheet and an associated magnetic flux rope and comparisons with ACE, *J. Geophys. Res.*, *107*(A11), 1365, doi:10.1029/2001JA009158.

Eastwood, J. P., et al. (2016), Ion-scale secondary flux ropes generated by magnetopause reconnection as resolved by MMS, *Geophys. Res. Lett.*, *43*, 4716–4724, doi:10.1002/2016GL068747.

Escoubet, C. P., M. Fehringer, and M. Goldstein (2001), Introduction: The Cluster mission, *Ann. Geophys.*, *19*, 1197–1200, doi:10.5194/angeo-19-1197-2001.

Forsyth, C., et al. (2008), Observed tail current systems associated with bursty bulk flows and auroral streamers during a period of multiple substorms, *Ann. Geophys.*, *26*, doi:10.5194/angeo-26-167-2008.

Forsyth, C., M. Lester, A. Fazakerley, C. Owen, and A. Walsh (2011), On the effect of line current width and relative position on the multi-spacecraft curlometer technique, *Planet. Space Sci.*, *59*, 598–605, doi:10.1016/j.pss.2009.12.007.

Haaland, S., B. O. Sonnerup, M. Dunlop, E. Georgescu, G. Paschmann, B. Klecker, and A. Vaivads (2004), Orientation and motion of a discontinuity from Cluster curlometer capability: Minimum variance of current density, *Geophys. Res. Letts.*, *31*, L10804, doi:10.1029/2004GL020001.

Haaland, S., J. Reistad, P. Tenfjord, J. Gjerloev, L. Maes, J. DeKeyser, R. Maggiolo, C. Anekallu, and N. Dorville (2014), Characteristics of the flank magnetopause: Cluster observations, *J. Geophys. Res. Space Physics*, *119*, 9019–9037, doi:10.1002/2014JA020539.

Henderson, P. D., C. J. Owen, A. D. Lahiff, I. V. Alexeev, A. N. Fazakerley, L. Yin, A. P. Walsh, E. Lucek, and H. Réme (2008), The relationship between j × B and ∇ ⊠ Pe in the magnetotail plasma sheet: Cluster observations, *J. Geophys. Res.*, *113*, A07S31, doi:10.1029/2007JA012697.

Nakamura, R., *et al.* (2008), Cluster observations of an ion-scale current sheet in the magnetotail under the presence of a guide field, *J. Geophys. Res.*, *113*, A07S1, doi:10.1029/2007JA012760.

Narita, Y., R. Nakamura, and W. Baumjohann (2013), Cluster as current sheet surveyor in the magnetotail, *Ann. Geophys.*, *31*, 1605–1610, doi:10.5194/angeo-31-1605-2013.

Panov, E., J. Büchner, M. Fränz, A. Korth, Y. Khotyaintsev, B. Nikutowski, S. Savin, K.-H. Fornaçon, I. Dandouras, and H. Reme (2006), CLUSTER spacecraft observation of a thin current sheet at the Earth's magnetopause, *Adv. Space Res.*, *37*(7), 1363–1372, doi:10.1029/2006GL026556.

Petrukovich, A., A. Artemyev, I. Vasko, R. Nakamura, and L. Zelenyi (2015), Current sheets in the Earth magnetotail: Plasma and magnetic field structure with Cluster project observations, *Space Sci. Rev.*, *188*, 311–337, doi:10.1007/s11214-014-0126-7.

Ritter, P., and H. Lühr (2013), Determining field-aligned currents with the Swarm constellation mission, *Earth Planets Space*, *65*, 1285–1294, doi:10.5047/eps.2013.09.006.

Robert, P., M. W. Dunlop, A. Roux, and G. Chanteur (1998), Accuracy of current density determination, in *Analysis Methods for Multispacecraft Data*, *ISSI Sci. Rep., SR-001*, 395–418, Kluwer Academic Pub., Dordrecht, Netherlands.

Roux, A., P. Robert, D. Fontaine, O. LeContel, P. Canu, and P. Louarn (2015), What is the nature of magnetosheath FTEs?, *J. Geophys. Res. Space Physics*, *120*, 4576–4595, doi:10.1002/2015JA020983.

Runov, A., et al. (2006), Local structure of the magnetotail current sheet: 2001 Cluster observations, *Ann. Geophys.*, *24*, 247–262, doi:10.5194/angeo-24-247-2006.

Shen, C., et al. (2008), Flattened current sheet and its evolution in substorms. *J. Geophys. Res.*, *113*, A07S21, doi:10.1029/2007JA012812.

Shen, C., J. Rong, M. Dunlop, Y. H. Ma, G. Zeng, and Z. X. Liu (2012), Spatial gradients from irregular, multiple-point spacecraft configurations, *J. Geophys. Res.*, *117*, A11207, doi:10.1029/2012JA018075.

Shen, C., et al. (2014), Direct calculation of the ring current distribution and magnetic structure seen by Cluster during geomagnetic storms, *J. Geophys. Res. Space Physics*, *119*, 2458–2465, doi:10.1002/2013JA019460.

Shi, J. K., et al. (2010), South-north asymmetry of field-aligned currents in the magnetotail observed by Cluster, *J. Geophys. Res.*, *115*, A07228, doi:10.1029/2009JA014446.

Shi, Q. Q., C. Shen, Z. Y. Pu, M. W. Dunlop, Q.-G. Zong, H. Zhang, C. J. Xiao, Z. X. Liu, and A. Balogh (2005), Dimensional analysis of observed structures using multipoint magnetic field measurements: Application to Cluster, *Geophys. Res. Letts.*, *32*, L12105, doi:10.1029/2005GL022454.

Shi, Q. Q., C. Shen, M. W. Dunlop, Z. Y. Pu, Q.-G. Zong, Z. X. Liu, E. Lucek, and A. Balogh (2006), Motion of observed structures calculated from multi-point magnetic field measurements: Application to Cluster, *Geophys. Res. Letts.*, *33*, L08109, doi:10.1029/2005GL025073.

Vallat, C., I. Dandouras, M. Dunlop, A. Balogh, E. Lucek, G. K. Parks, M. Wilber, E. C. Roelof, G. Chanteur, and H. Rème (2005), First current density measurements in the ring current region using simultaneous multi-spacecraft CLUSTER-FGM data, *Ann. Geophys.*, *23*, 1849–1865, doi:10.5194/angeo-23-1849-2005.

Vogt, J., A. Albert, and O. Marghitu (2009), Analysis of three-spacecraft data using planar reciprocal vectors: methodological framework and spatial gradient estimation, *Ann. Geophys.*, *27*, 3249–3273, doi:10.5194/angeo-27-3249-2009.

Vogt, J., E. Sorbalo, M. He, and A. Blagau (2013), Gradient estimation using configurations of two or three spacecraft, *Ann. Geophys.*, *31*, 1913–1927, doi:10.5194/angeo-31-1913-2013.

Xiao, C. J., Z. Y. Pu, Z. W. Ma, S. Y. Fu, Z. Y. Huang, and Q. G. Zong (2004), Inferring of flux rope orientation with the minimum variance analysis technique, *J. Geophys. Res.*, *109*, A11218, doi:10.1029/2004JA010594.

Zhang, Q.-H., et al. (2011), The distribution of the ring current: Cluster observations, *Ann. Geophys.*, *29*, 1655–1662, doi:10.5194/angeo-29-1655-2011.